

Are your MRI contrast agents cost-effective?

Learn more about generic Gadolinium-Based Contrast Agents.



**FRESENIUS
KABI**

caring for life

AJNR

Rhabdomyosarcoma of the head and neck in adults: MR and CT findings.

J H Lee, M S Lee, B H Lee, D H Choe, Y S Do, K H Kim, S Y Chin, Y S Shim and K J Cho

AJNR Am J Neuroradiol 1996, 17 (10) 1923-1928

<http://www.ajnr.org/content/17/10/1923>

This information is current as
of April 18, 2024.

Rhabdomyosarcoma of the Head and Neck in Adults: MR and CT Findings

Jeong Hoon Lee, Mi Sook Lee, Byung Hee Lee, Du Hwan Choe, Young Soo Do, Kie Hwan Kim, Soo Yil Chin, Youn Sang Shim, and Kyung-Ja Cho

PURPOSE: To evaluate imaging findings of rhabdomyosarcoma of the head and neck in adults.

METHODS: We examined 11 patients (seven men and four women; 17 to 73 years old) with pathologically proved rhabdomyosarcoma of the head and neck. The tumors originated in the paranasal sinuses (n = 6), cheek (n = 3), nasal cavity (n = 1), and infratemporal fossa (n = 1). Eight of the rhabdomyosarcomas were of the embryonal type, two were pleomorphic, and one was alveolar. Necrosis was seen in four patients, but calcification or intratumoral hemorrhage was not found. Two tumors had nodal extension. Contrast-enhanced CT was performed in 10 patients, and two patients had contrast-enhanced MR imaging. **RESULTS:** On CT scans, the masses enhanced to the same degree as adjacent muscle. The masses showed a homogeneous pattern in six cases and a heterogeneous pattern in four cases. The tumor margins were poorly defined in eight cases. On MR images, the masses were homogeneously isointense with muscle on T1-weighted studies and were hyperintense relative to muscle on T2-weighted studies. On both CT and MR images, 10 of 11 cases showed poorly defined, homogeneous masses destroying adjacent bony structures. **CONCLUSIONS:** MR imaging seems to be better than CT for initial and follow-up examination of patients with rhabdomyosarcoma because of its multiplanar capability and because it more precisely defines the extent of tumor.

Index terms: Head, neoplasms; Neck, neoplasms; Myosarcoma

AJNR Am J Neuroradiol 17:1923–1928, November 1996

Rhabdomyosarcoma is one of the most common soft-tissue sarcomas in children under 15 years of age, and the head and neck is the principal location for childhood rhabdomyosarcoma; however, head and neck rhabdomyosarcoma is rare in adults (1–3). There is also a general impression that the tumor has a different natural course, response to treatment, and prognosis in adults than in children (3–5). Reports of rhabdomyosarcoma of the head and neck in adults have been included in general series of imaging findings of rhabdomyosar-

coma (6–8); we describe the computed tomographic (CT) and magnetic resonance (MR) imaging findings of rhabdomyosarcoma of the head and neck in a group composed exclusively of adults.

Materials and Methods

Eleven patients with histopathologically proved rhabdomyosarcoma of the head and neck had CT or MR imaging over a 5-year period. The patients included seven men and four women who were 17 to 73 years old (median, 29 years). Ten patients had CT after receiving an intravenous bolus injection of 150 mL of contrast material. The CT scans were obtained with 5-mm-thick contiguous sections in the axial plane. Coronal studies were performed in five cases to assess intraorbital or intracranial extension. MR images were obtained in two patients on a 1.0-T unit with spin-echo T1-weighted pulse sequences of 500/20/3 (repetition time/echo time/excitations) and T2-weighted sequences of 2000/80/1 in the axial plane. The section thickness was 6 mm with a 2-mm gap. The acquisition matrix was 256 × 256 with a field of view of 15 mm. After intravenous injection of gadopentetate dimeglumine

Received June 30, 1995; accepted after revision May 28, 1996.

From the Departments of Diagnostic Radiology (J.H.L., M.S.L., B.H.L., D.H.C., Y.S.D., K.H.K., S.Y.C.), Otolaryngology-Head and Neck Surgery (Y.S.S.), and Anatomic Pathology (K-J.C.), Korea Cancer Center Hospital, Seoul.

Address reprint requests to Jeong Hoon Lee, MD, Department of Diagnostic Radiology, Korea Cancer Center Hospital, 215–4, Gongneung-dong, Nowon-gu, Seoul 139–240, Korea.

AJNR 17:1923–1928, Nov 1996 0195-6108/96/1710–1923

© American Society of Neuroradiology

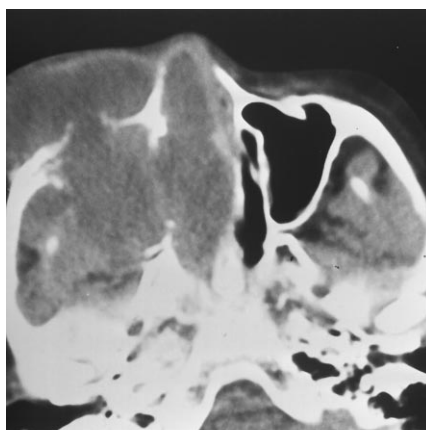
TABLE 1: Patient data, tumor characteristics, and clinical course in 11 adults with head and neck rhabdomyosarcoma

Patient	Age, y/ Sex	Location of Tumor	Cell Type	Size, cm	Tumor Extent	Clinical Course
1	17/F	MS	Embryonal	7.5	ES, NC, O, OC	Alive; NED>2 y
2	17/F	MS	Embryonal	7.0	ES, NC, O	Alive; NED>2 y
3	32/M	MS	Pleomorphic	4.0	NC, O	Alive but with disease
4	73/M	MS	Pleomorphic	7.5	O, NC	Alive but with disease
5	26/M	ES	Embryonal	7.0	MS, O, IC	Metastases to lung and bone Died of progressive disease
6	49/F	ES	Embryonal	3.5	MS	Nodal extension
7	36/M	NC	Alveolar	4.0	MS, ES	Nodal extension
8	32/F	ITF	Embryonal	7.5	IC	Alive but with disease
9	20/M	Cheek	Embryonal	7.4	Confined to cheek	Metastases to lung and heart
10	29/M	Cheek	Embryonal	7.0	O, NC, OC	Died of progressive disease
11	29/M	Cheek	Embryonal	11.0	MS, OC	Died of progressive disease

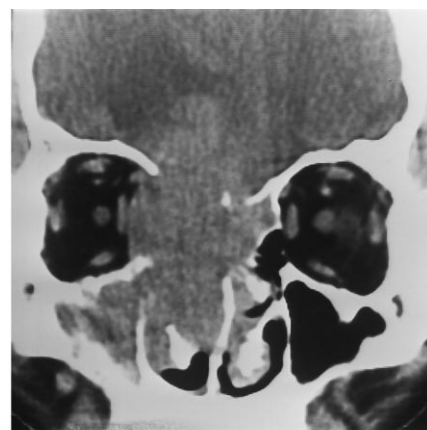
Note.—NED indicates no evident disease; ES, ethmoidal sinus; IC, intracranial; ITF, infratemporal fossa; MS, maxillary sinus; NC, nasal cavity; O, orbit; and OC, oral cavity.

Fig 1. Embryonal rhabdomyosarcoma of the maxillary sinus. Contrast-enhanced axial CT scan shows a homogeneous mass that originates from the right maxillary sinus and extends to the nasal cavity and the cheek. The mass shows slightly lower density than surrounding muscle. All maxillary sinus walls are destroyed.

Fig 2. Embryonal rhabdomyosarcoma of the ethmoidal sinus. Contrast-enhanced coronal CT scan shows a homogeneous mass in the right ethmoidal sinus and destruction of surrounding bony structures. The mass extends to the nasal cavity, anterior cranial fossa, and orbit. It is not clear whether the opacification of the right maxillary sinus is due to trapped secretion or direct extension of the tumor.



1



2

(0.1 mmol/kg body weight), T1-weighted axial and coronal images were obtained. The imaging findings were reviewed retrospectively to evaluate points of tumor origin, homogeneity, marginal definition, density/signal intensity, bone destruction, calcification, hemorrhage, necrosis, and nodal extension. The densities/signal intensities of the tumors were compared with those of muscle. In cases of heterogeneous masses, the lesions were characterized by the predominant density/signal intensity. Lymph nodes that were greater than 10 mm in minimal axial diameter were considered indicative of nodal extension (9). Two patients underwent surgery and the others had a biopsy or aspiration biopsy cytology.

Results

Patient data, site of tumor origin, cell type, size and extent of tumor, and clinical course are itemized in Table 1.

Six tumors arose in the paranasal sinuses. Four of these arose in the maxillary sinus and two in the ethmoidal sinus. CT scans showed a poorly defined homogeneous mass that destroyed adjacent bony structures and extended to surrounding spaces (Figs 1 and 2). After intravenous administration of contrast material, the masses enhanced to the same degree as surrounding muscle in four cases, became slightly hyperdense in one case, and became slightly hypodense in one case. None of these showed necrosis. Nodal extension (to internal jugular and spinal accessory chains) was seen in only one case (in a tumor of the ethmoidal sinus with embryonal type cells). One tumor that arose in the maxillary sinus was also examined by MR imaging, which revealed a homoge-

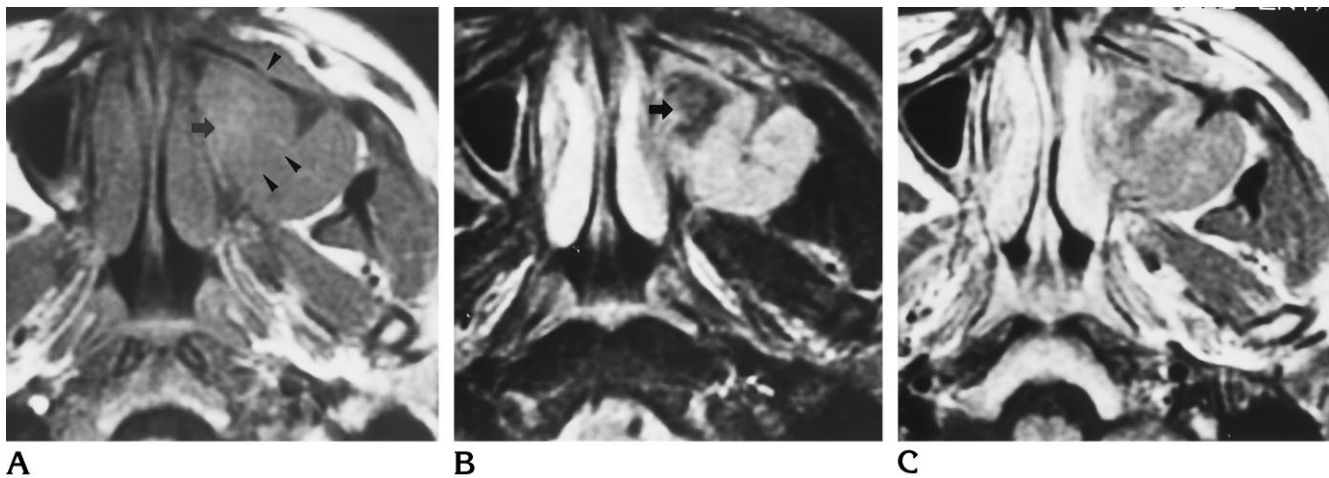


Fig 3. Pleomorphic rhabdomyosarcoma of the maxillary sinus.

A, Axial T1-weighted image (500/20) shows a mass that originates from the left maxillary sinus and extends outside the sinus. The mass shows homogeneous signal isointensity with surrounding muscle, with areas of subtle hyperintensity (arrow). The maxillary sinus walls appear thin and discontinuous (arrowheads).

B, Axial T2-weighted image (2000/80) shows a hyperintense mass with areas of dark signal intensity (arrow).

C, Contrast-enhanced MR image shows enhancement of portions of the mass.

neous mass on all pulse sequences (Fig 3). Signal intensity of the mass was isointense with surrounding muscle on T1-weighted images and hyperintense on T2-weighted images; therefore, tumor extent was defined better on the T2-weighted sequences than on T1-weighted sequences or CT scans. After administration of contrast material, the mass enhanced slightly more than surrounding muscle. Trapped secretion between the mass and the sinus wall was distinguishable from tumor; it was slightly hyperintense on the T1-weighted sequence (Fig 3A) and hypointense on the T2-weighted sequence (Fig 3B) and did not show enhancement (Fig 3C). On the CT study, it was difficult to differentiate trapped secretion and direct extension of tumor.

Bone destruction of the maxillary sinus was also well shown by MR imaging. Cortical dark signal of the maxillary sinus wall was slight on T1-weighted images and discontinuous on T2-weighted images and on contrast-enhanced sequences. A soft-tissue mass on the other side of the sinus wall was an additional finding of bony destruction.

Three tumors arose in the cheek. All were bulky masses up to 11 cm in diameter, with a large portion of them located in the region of the cheek. Two of these tumors were imaged by CT, and appeared as poorly defined, heteroge-

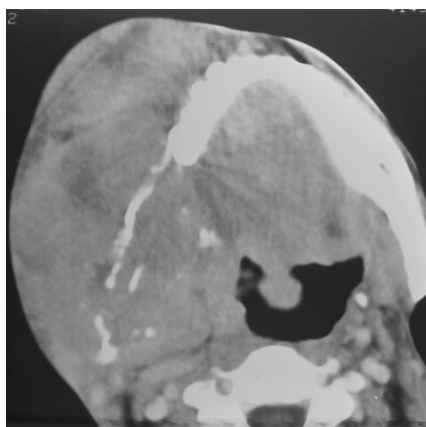
neous, and isodense masses with focal hypodense lesions that were believed to be necrosis (Fig 4). In one case, there was evidence of destruction of the mandible, and the tumor extended to the oral cavity and maxillary sinus. The other patient had MR imaging, which showed a well-defined, homogeneous mass with the same signal intensity as the tumor shown in Figure 3. Also evident at MR imaging were extension of the mass into the orbit, nasal cavity, and oral cavity, and discontinuity of the dark signal of cortical bone.

One tumor arose in the infratemporal fossa. In this case, a CT scan showed a well-marginated, heterogeneous, isodense mass with small foci of low attenuation, suggesting necrosis (Fig 5). The mass destroyed the skull base and extended to the middle cranial fossa.

One tumor arose in the nasal cavity. Here, a CT scan showed a poorly defined, heterogeneous, isodense mass that extended to the ethmoidal and maxillary sinuses. Nodal extension was demonstrated in the internal jugular and submandibular chains. Lymph node biopsy was performed and confirmed the presence of tumor.

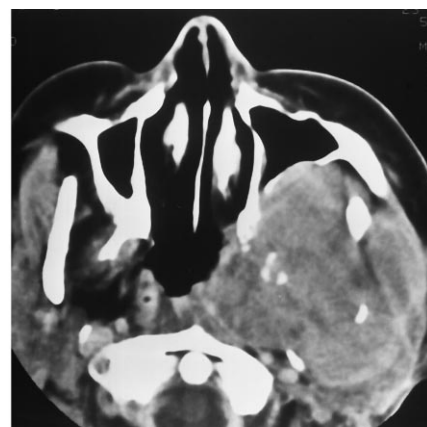
Calcification or intratumoral hemorrhage was not found in any case, but microscopic examination revealed focal areas of hemorrhage in two cases in which surgery was performed.

Fig 4. Embryonal rhabdomyosarcoma of the cheek. Postcontrast axial CT scan shows a poorly defined, heterogeneous mass in the right cheek with destruction of the mandibular ramus.



4

Fig 5. Embryonal rhabdomyosarcoma of the infratemporal fossa. Contrast-enhanced axial CT scan shows a well-margined, heterogeneous mass in the left infratemporal fossa and destruction of surrounding bony structures.



5

TABLE 2: Anatomic distribution of adult rhabdomyosarcoma during a 5-year period at the Korea Cancer Center Hospital (51 cases)

Anatomic Location	n	%
Head and neck	11	22
Paranasal sinuses	6	12
Cheek, infratemporal fossa	4	8
Nasal cavity	1	2
Trunk	22	43
Chest wall, back, flank	7	14
Buttock, inguinal	6	12
Testicle, prostate	6	12
Uterus, cervix	3	6
Extremity	18	35
Upper limb	9	18
Lower limb	9	18
Total	51	100

Discussion

Rhabdomyosarcoma is the most common soft-tissue sarcoma not only of children under 15 years of age but also of adolescents and young adults (1). The head and neck, especially the orbit, is the most frequent site of childhood rhabdomyosarcoma; but this location is rare in adults (1–3). The incidence and location of adult rhabdomyosarcomas seen at our institution over a 5-year period are given in Table 2. In adults, the head and neck region is affected less commonly than in children, but the extremities are affected more commonly. In contrast to childhood rhabdomyosarcoma of the head and neck, all tumors in our adult patients were located in nonorbital regions, and 73% of the tumors were in parameningeal locations. The ethmoidal sinus is the most common site of origin of head and neck rhabdomyosarcoma in adults (3). In our series, the most common site of

origin was the maxillary sinus, seen in four (36%) of the 11 patients. Rhabdomyosarcoma of the ethmoidal sinus is associated with a poor prognosis, because the tumor's location in the parameningeal region makes it likely to invade the meninges. It is noteworthy that in our series, two of three patients with rhabdomyosarcoma of the cheek died of tumor progression, and distant metastases developed in the third. We think the reason for this poor outcome was the large size of the tumors (mean, 8.5 cm) or the lack of a bony barrier.

Histologically, rhabdomyosarcomas are classified into four types: embryonal, botryoid, alveolar, and pleomorphic (1, 2). The embryonal type is the most common and accounts for 70% to 80% of all rhabdomyosarcomas. It affects mainly but not exclusively children between birth and 15 years of age and occurs predominantly about the head and neck, the genitourinary tract, and the retroperitoneum. The botryoid type is a variant of the embryonal type. Alveolar rhabdomyosarcoma is less frequent; it accounts for 10% to 20% of all rhabdomyosarcomas and affects chiefly children and young adults between 10 and 25 years of age. Pleomorphic rhabdomyosarcoma is actually the least common type in general, but the predominant type in adults. It may occur at any age but probably has its peak prevalence in patients older than 45 years. It is primarily a tumor of the large muscles of the extremities. Previously reported cases have shown a relatively high frequency of the alveolar type in adult rhabdomyosarcoma of the head and neck (3, 4), but, in our series, the predominant tumors (73%) were the embryonal type. It is impossible to compare

imaging findings of each subtype in our series because our sample is so small; nor were we able to compare the imaging findings with pathologic results, since most patients were treated with chemotherapy and/or radiation therapy.

Along with tumor invasiveness, metastasis, and regional lymph node involvement, age at diagnosis is a predictor of outcome in patients with rhabdomyosarcoma. Overall survival is worse for adults than for children (10).

The extent of bone erosion has been suggested to be an important prognostic factor in nonorbital rhabdomyosarcoma of the head and neck (11). Major sites of metastases are the lung, lymph nodes, and bone marrow, followed by the heart, brain, and meninges (1). The frequency of nodal metastasis is 7% to 50% in general and less common for tumors located in the head and neck (3, 6, 7, 10, 12), but there is no evidence of a relationship between lymphatic spread and age, sex, or histologic subtype (12). In our series, distant metastases (lung, bone, and heart) developed in two patients with ethmoidal and cheek rhabdomyosarcoma. In one patient, local recurrence developed 2 months after surgery, and three patients died of progressive disease.

CT findings of head and neck rhabdomyosarcoma have been described as showing poorly defined, inhomogeneous soft-tissue masses destroying adjacent bone (6, 8). In our series, most of the CT studies showed poorly defined, relatively homogeneous masses with destruction of adjacent bony structures. After intravenous injection of contrast material, the masses enhanced generally to the same degree as muscle. Necrosis was an uncommon finding, and hemorrhage or calcification was not seen. These findings were not different from those of Latack et al (6).

The most commonly reported MR imaging appearance of rhabdomyosarcoma in the head and neck is that of a homogeneous mass, isointense or minimally hyperintense relative to muscle on T1-weighted images and hyperintense relative to both muscle and fat on T2-weighted images, with postcontrast images showing enhancement of the tumor (7). Our findings mirror this description. The hallmark of bony destruction on MR images (ie, loss of normal dark signal of cortical bone and/or a hyper-

intense mass on the other side of the bone) was seen without difficulty on T2-weighted and enhanced MR images, as in Figure 3.

Rhabdomyosarcomas of the head and neck in adults are different from those of childhood in their site of origin (3), but they produce similar imaging findings (6–8). Malignant tumors in the head and neck in adults also show similar imaging findings, but lymphoma is somewhat different from rhabdomyosarcoma in its multifocal involvement and is less often associated with invasion and destruction of adjacent bony structures (13, 14). Liposarcomas usually have a component of fat density/intensity. Chordoma, chondrosarcoma, and osteosarcoma have areas of calcification. Other malignant tumors of the head and neck, such as squamous cell carcinomas, usually have imaging findings similar to those of rhabdomyosarcoma (15, 16), but age at diagnosis of rhabdomyosarcoma is younger than that for squamous cell carcinoma, which may prove helpful in the differential diagnosis. MR imaging seems to be better than CT for initial and follow-up examination of rhabdomyosarcoma because of its multiplanar capability and ability to precisely define the extent of tumor.

References

1. Enzinger FM, Weiss SW. Rhabdomyosarcoma. In: *Soft Tissue Tumors*. 2nd ed. St Louis, Mo: Mosby; 1988:448–488
2. Feldman BA. Rhabdomyosarcoma of the head and neck. *Laryngoscope* 1982;92:424–440
3. Nayar RC, Prudhomme F, Parise O Jr, Gandia D, Lubinski B, Schwaab G. Rhabdomyosarcoma of the head and neck in adults: a study of 26 patients. *Laryngoscope* 1993;103:1362–1366
4. Nakhleh RE, Swanson PE, Dehner LP. Juvenile (embryonal and alveolar) rhabdomyosarcoma of the head and neck in adults: a clinical, pathologic, and immunohistochemical study of 12 cases. *Cancer* 1991;67:1019–1024
5. Lloyd RV, Hajdu SI, Knapper WH. Embryonal rhabdomyosarcoma in adults. *Cancer* 1983;51:557–565
6. Latack JT, Hutchinson RJ, Heyn RM. Imaging of rhabdomyosarcomas of the head and neck. *AJNR Am J Neuroradiol* 1987;8:353–359
7. Yousem DM, Lexa FJ, Bilaniuk LT, Zimmerman RI. Rhabdomyosarcoma in the head and neck: MR imaging evaluation. *Radiology* 1990;177:683–686
8. Ng YY, Kingston JE, Perry NM, Reznick RH. The role of computerized tomographic scanning in the management of rhabdomyosarcoma in nonorbital head and neck sites. *Pediatr Hematol Oncol* 1990;7:149–157
9. Van den Brekel MWM, Stel HV, Castelijns JA, et al. Cervical lymph node metastasis: assessment of radiologic criteria. *Radiology* 1990;177:379–384

10. La Quaglia MP, Heller G, Ghavimi F, et al. The effect of age at diagnosis on outcome in rhabdomyosarcoma. *Cancer* 1994;73:109–117
11. Mandell LR, Massey V, Ghavimi F. The influence of extensive bone erosion on local control in non-orbital rhabdomyosarcoma of the head and neck. *Int J Radiol Oncol Biol Phys* 1989;17:649–653
12. Lawrence W Jr, Hays DM, Heyn R, et al. Lymphatic metastases with childhood rhabdomyosarcoma: a report from the intergroup rhabdomyosarcoma study. *Cancer* 1987;60:910–915
13. Lee YY, Tassel PV, Nauert C, North LB, Jing BS. Lymphomas of the head and neck: CT findings at initial presentation. *AJNR Am J Neuroradiol* 1987;8:665–671
14. Depena CA, Tassel PV, Lee YY. Lymphoma of the head and neck. *Radiol Clin North Am* 1990;28:723–743
15. Hasso AN. CT of tumors and tumor-like conditions of the paranasal sinuses. *Radiol Clin North Am* 1984;22:119–130
16. Kondo M, Horiuchi M, Shiga H, et al. Computed tomography of malignant tumors of the nasal cavity and paranasal sinuses. *Cancer* 1981;50:226–231